Colloid Polym Sci 277:601–606 (1999)

SHORT COMMUNICATION

T. Okubo
A. Tsuchida
H. Yoshimi
H. Maeda

Rotational diffusion of anisotropic-shaped colloidal particles in microgravity as studied by free-fall experiments

Received: 10 November 1998
Accepted in revised form: 22 December 1998

T. Okubo (✉) · A. Tsuchida
H. Yoshimi · H. Maeda
Department of Applied Chemistry
Gifu University, Gifu 501-1193, Japan
e-mail: okubotsu@apchem.gifu-u.ac.jp
Fax: +81-58-2932628

Abstract Rotational relaxation times (τ) and diffusion coefficients of ellipsoidal colloids of tungstic acid are studied in aqueous suspension in microgravity by free-fall experiments. τ values are evaluated from the relaxation traces of the optical transmittance of the suspension using the stopped-flow technique. Experimental errors at 0 *G* are small compared with those at 1 *G*, which is ascribed to lack of the movement of impurities in suspension such as quite small dust and bubbles and the convection of the suspension in microgravity. The limiting slopes of the relaxation curves in the plots of the transmittance against time at 1 *G* depend on the flow direction of the suspension in the flow cell, whereas those at 0 *G* remain zero irrespective of the flow direction. For more reliable diffusion coefficients are obtained in microgravity; however, the diffusion coefficients themselves are quite insensitive to gravity.

Key words Rotational diffusion – Rotational relaxation time – Tungstic acid colloid – Microgravity effects – Free-fall experiments

Introduction

A gravitational field is one of the important parameters for the physico-chemical properties of colloidal dispersion systems [1–3]. Because of the difficulty to attain zero gravity on the earth most of the experimental studies have been made in gravity. Vanderhoff et al. [4] succeeded in preparing monodispersed polystyrene spheres 5–18 μm in diameter with narrower particle size distributions in microgravity than those prepared in gravity. A series of polyacrylamide gels have been synthesized in microgravity [5]. Quite recently Zhu et al. [6] reported the microgravity effect on the morphology of colloidal crystals using the space shuttle Columbia. We are interested in the microgravity effect for colloidal dispersion systems. Recently, the crystal growth rates of colloidal crystals and the formation rates of colloidal silica spheres themselves have been measured in microgravity by parabolic flights of an aircraft [7, 8]. In these works substantial decreases in the rates were observed in microgravity.

In this report, rotational relaxation times (τ) and diffusion coefficients (D_r) of ellipsoidal colloids of tungstic acid are determined in aqueous suspension under microgravity by free-fall experiments. D_r is one of the fundamental properties of spherical and anisotropic colloids in suspension. Flow birefringence, non-Newtonian flow, electric birefringence, fluorescence depolarization and dielectric dispersion are typical methods that have been used for the determination so far [9–13]. Okubo [14] has proposed a stopped-flow technique as a new and convenient method for determining τ (ranging from 1 ms to several seconds) for anisotropic colloidal particles such as ellipsoidal colloids of tungstic acid. The important role of the electrical double layers on rotational diffusion has been clarified.

Under gravity exact values of τ are difficult to measure due to the sedimentation of anisotropic colloids and the convection of the suspension, since the downward sedimentation should occur which is accompanied with the birefringence flow. Monodispersed ellipsoidal colloids of tungstic acid have many advantages for the

study of rotational relaxations, such as chemical stability, uniformity in their size, etc. The duration of the microgravity obtained by the present free-fall facility is short (4.5 s); however, the size of the tungstic acid colloids is quite appropriate for the free-fall experiments.

We should note here that the gravitational effect is quite significant for translational and rotational diffusion. The ratio of the time of sedimentation of a sphere against that of diffusion, which is called the Péclet number, P_e is given by [15]

$$P_e = rS/D_t = (4\pi r^4 \Delta\rho\ g)/(3k_B T) \quad (1)$$

where r is the sphere radius, $\Delta\rho$ the difference in density between sphere and solvent, g the gravitational acceleration, η the viscosity of the solvent, k_B the Boltzman constant and T the absolute temperature, respectively. For tungstic acids, the Péclet number is estimated to be about 230 when a sphere of 1.5 μm radius and specific gravity of 5.5 are assumed in water suspension. The Péclet number estimated shows that the contribution of sedimentation is much larger than that of diffusion. The sedimentation of nonspherical particles such as tungstic acid colloids is complicated by the fact that the translational and rotational motions are coupled. The particles sediment in a direction that depends on their orientation. Rotational Brownian motion changes the orientation of the particles and hence their sedimentation speeds and directions; however, on average, the particles will move in the direction of gravity only. For homogeneous particles the average sedimentation velocity equals that of spherical particles. In conclusion, the microgravity effect on the rotational and translational motion is strong enough for the tungstic acid particles studied in this work.

Experimental

Rotational-relaxation-time (τ) measurements

The τ values are measured from the traces of the optical transmittance with time just after stopping the flow using a device as shown in Fig. 1. The instrument consists of a quartz flow cell (inner size $1 \times 5 \times 40$ mm), a solenoid valve, Phamed tubes (inner diameter 3.1 mm) and a peristaltic pump (Masterflex, 7524-10, Ill.). The pump circulates the colloidal suspension (about 40 ml) at a flow rate of 30 ml/min. Light from a light-emitting diode (LED, Sansui, 12 V, 600–800 nm) passes through the cell and the transmittance intensity is measured by a photodiode (Hamamatsu Photonics, S2281-01, Hamamatsu). In order to compensate for the light intensity fluctuation from the light source, a half mirror and another photodiode are equipped to monitor the absolute intensity of the LED. The signals from the photodiodes are led into preamplifiers (Hamamatsu, C2719) and then into homemade offset main amplifiers. The total rise time of the instrument is less than 7 μs. The signals are finally recorded on an A/D converter [Contec, AD12-8(PM), Osaka, 10 μs interval] in a personal computer (NEC, PC9821, Tokyo) and for safety on another A/D converter of the free-fall facility. The signal is recorded from 2 s before dropping to

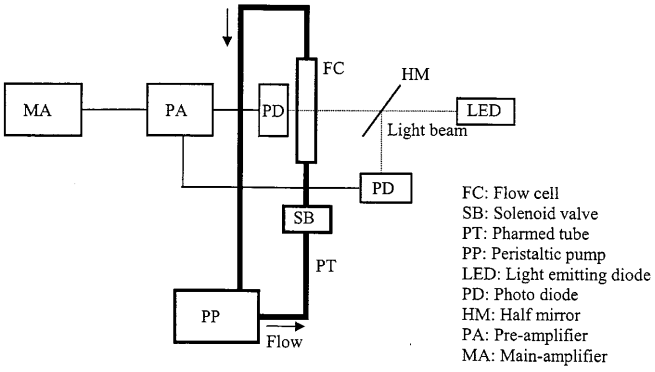

Fig. 1 Block diagram of the instrument for the measurements of the rotational diffusion constants of colloidal particles

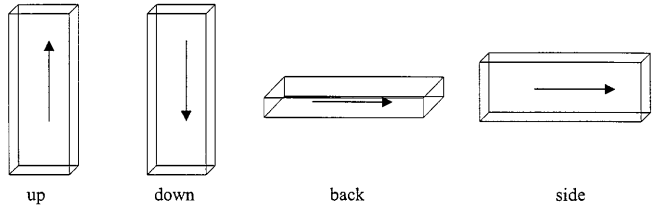

Fig. 2 Directions of the sample flow

12 s after stopping the free-fall capsule. All the optical components are fixed tightly in a firm aluminum measurement box.

The flow directions of the sample suspension in the observation cell are shown in Fig. 2. For the four flow directions (abbreviated as "up", "down", "back" and "side") τ values were observed for both 1 G and 0 G experiments. The probing light always passed through the cell perpendicular to the largest plane.

It should be mentioned here that a halogen lamp was used first as the light source for the measurements. It was found, however, that the light intensity of the lamp increased substantially (about 10–20%) as soon as microgravity was achieved, which is undoubtedly due to the lack of cooling of the bulb surface and/or the filament by convection. The light intensity of the LED was quite insensitive to gravity.

The microgravity experiments were performed using free-fall facility of the Micro-Gravity Laboratory of Japan (MGLAB) in Toki, Gifu. The duration of the microgravity was about 4.5 s. G values during the free fall were ± 0.0003 for both horizontal and vertical directions. Change in temperature, humidity and pressure inside the capsule at 0 G were small, ± 0.1 °C, ± 0.2%RH and ± 0.0015 kg/cm^2, respectively.

Materials

Monodispersed ellipsoidal colloids of tungstic acid were prepared and purified by the method of Furusawa and Hachisu [16]. 1 N HCl (25 ml) (Wako Pure Chemicals, Osaka) and 50 ml 7 wt% Na_2WO_4 (>99%, Wako) were kept at 0–5 °C separately for more than 10 h before mixing. The two solutions were then mixed completely, and again refrigerated for more than 10 h. A slightly yellowish gel of tungstic acid colloids was obtained. The gel was poured into 200 ml water, and then the suspension was stirred thoroughly. The suspension thus obtained was centrifuged (Kokusan, type H-9R, Tokyo) at 5000–6000 rpm for 480 s. The

dispersing and the centrifuging were repeated 5 times, and the suspension (1.2 l) was incubated in a thermostated bath (changed from 0 to 30 °C) for more than 12 h. Then the monodispersed crystalloids appeared. The colloids were further purified by repeated decantation.

Lengths of the major axis ($2c$) and the middle one ($2b$) were determined by a reversed-type metallurgical microscope (Olympus, PME3, Tokyo, ×400–1000). The cell used was the same as that described in a previous paper [14]. The average values of $2c$ and $2b$ were 3.6 μm (standard deviation δ_{2c} = 0.25 μm) and 2.2 μm (δ_{2b} = 0.26 μm), respectively.

The tungstic acid colloids were also obtained by incubation in an aqueous ethylene glycol mixture, and were small compared with those prepared in water. The length of the minor axis ($2a$) was not determined experimentally in this work but was estimated from the data of previous work [16] on electrophoresis measurements on the same colloids. The colloidal samples thus prepared were monodispersed and ellipsoidal. $2a$ values were between 0.01 and 0.09 μm [17–19]. For the W29 colloids $2a$ was evaluated to be 0.075 μm. τ should be very insensitive to the $2a$ value.

The relationship between the $2b$ and $2c$ values of the colloidal samples prepared in this (○) and previous (×) [14] work is shown in Fig. 3. The linear line indicates the least-squares fit for the previous values and the relation of $b = 0.41c$ held. Theoretical τ values using Perrin's equation [20] were calculated from the $2c$ values observed and the $2b$ values were estimated from the relation $b = 0.41c$. Note that Suda and Imai [21] reported a relation of $b = 0.30c$ for the same colloids, though their photographs showed a thin rectangle instead of an ellipsoid. Furusawa and Hachisu [17, 18] have reported the transformation of shape from ellipsoidal to rectangular with time.

The water used for the preparation of the sample suspensions was obtained from a Milli-Q water system (Millipore Ltd., Milli-RO Plus and Milli-Q Plus, Bedford, Mass.). Ethylene glycol was the purest grade available from Wako Chemicals. Special care was taken to avoid contaminating the suspension with ionic impurities.

Results and discussion

Methods

The ellipsoidal colloids of tungstic acid are oriented along the flow direction during continuous flow due to the shearing forces arising from the velocity gradient. When the solution flow is stopped, the colloidal particles revert to rotating freely in a Brownian random distribution. Translational diffusion is not very significant in the stopped-flow method, since the flow of the solvent molecules stops completely when the observation starts. For large ellipsoidal colloids, the multiple scattering of light changes significantly with orientation. Thus, the transmittance would relax toward an equilibrium point after the stopped-flow.

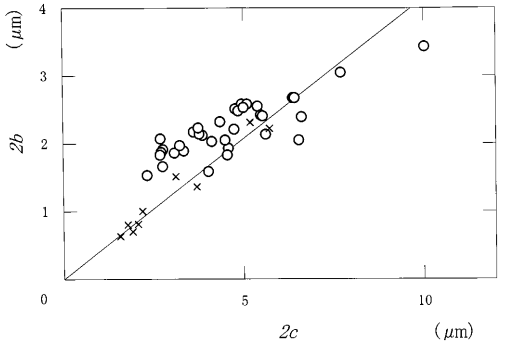

Fig. 3 Relationship between the axis (c) and middle axes (b) of tungstic acid colloids.○ :W1-W37, this work, ×: taken from Ref. [14]

The rotational diffusion constant, D_r, is obtained directly from the observed τ values by using Eq. (2).

$$D_r = 1/6\tau \ . \tag{2}$$

The theoretical values of D_r of ellipsoids are obtained from Perrin's equations without any assumptions if three axes are given [20].

$$D_r = 3kT\left(a^2P + b^2Q\right)/16\pi\eta\left(a^2 + b^2\right) \tag{3}$$

$$P = \int_0^\infty \mathrm{d}s \Big/ \left(a^2 + s\right)\sqrt{(a^2 + s)(b^2 + s)(c^2 + s)} \tag{4}$$

$$a^2P + b^2Q + c^2R = \int_0^\infty \mathrm{d}s \Big/ \sqrt{(a^2 + s)(b^2 + s)(c^2 + s)} \tag{5}$$

$$P + Q + R = 2/abc, \quad a < b < c \tag{6}$$

where a, b and c denote the lengths of the minor, middle and major axes of an ellipsoidal colloid, respectively. The constants P, Q and R are derived from Eqs. (3)–(6). k, T and η in Eq. (3) are the Boltzmann constant, the absolute temperature and the viscosity of the solvent, respectively.

For small colloidal particles the observed values of τ were somewhat larger than the calculated ones [14]. Since the experiments were performed in the absence of foreign salt, the thickness of the electrical double layer (D_l) given by $1/\kappa$ (κ is the Debye parameter) should be taken into account in the evaluation of the effective size of the colloids, i.e., the effective values of the minor, middle and major axes, respectively.

$$D_l = (4\pi Bn)^{-1/2} \ , \tag{7}$$

where B is the Bjerrum length ($e^2/\epsilon\, kT$, 7.19 Å at 25 °C) and n is the concentration of "free" (not bound to macroions) cations and anions in suspension. e and ε are the electronic charge and the dielectric constant of the solvent, respectively. In the absence of foreign salt, n corresponds to the "free" counterions (hydronium ions). The importance of the "electrostatic" inter-macroion repulsion and the electrical double layers has often been pointed out for the physico-chemical properties of various colloidal suspensions, especially in salt-free systems [22–25]. The double layers are so soft that they are deformed and even stripped away quite easily by the shearing forces.

Reference experiments in gravity

An example of the traces of the optical transmittance caused by the rotational relaxation of W29 colloidal particles at 1 G for the upward, "up" flow direction is shown in Fig. 4. The ordinate designates the output voltage from a main amplifier. A large output means a large transmitted-light intensity, and the value in figures includes the offset from the absolute output. At $t = 0$ the suspension flow stopped within 0.1 s of stopping the pump, $t = 0$, which was confirmed by video-tape observation. During the suspension flow the colloidal particles are oriented along the flow direction. The large optical intensity and its pulse are seen in the figure. After stopping the pump the output decreased. Around $t = 3$ s, the output converged to the limiting value, which indicates that almost random orientation of the colloidal particles is attained. The straight line in the figure shows the least-squares linear fit of the output between $t = 4$–4.5 s. It is interesting to note that the slopes were sensitive to the flow directions. After subtracting the values of the linear–fit line from those of the original curve, the values were fitted by an exponential function and a vertical shift. The broken line shows the least-squares fit, and the rotational relaxation time τ is obtained.

The slopes of the limiting equilibrium lines at 1 G are shown in Fig. 5. The small dots and open circles indicate the measured and the average values for each flow direction. The average slopes were negative for "up", "down" and "back" directions, whereas that for "side" was positive. The transmitted-light measurements were made using the slender rectangular cell, central 8 mm in length and 40 mm in width. If the number of colloidal particles in the observation area in the cell decreases due to sedimentation by gravity, the intensity should increase and then the slope becomes positive. Furthermore, the downward movement of the particles caused by gravity may result in the particle orientation. For

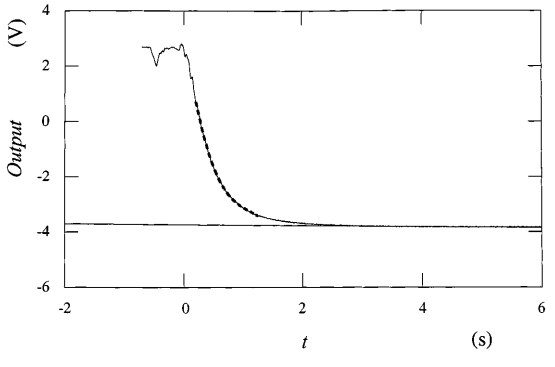

Fig. 4 Rotational relaxation curve of W29 particles at 22.6 °C. At 1 G, 0.20 wt%, "up" flow. *Solid line*: equilibrium linear fitting, *broken line*: exponential fitting

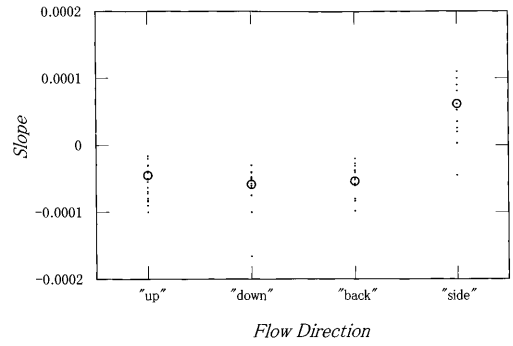

Fig. 5 Slope of the final equilibrium lines in the rotational relaxations of W29 particles at 1 G. 0.20 wt%, ○ : average values

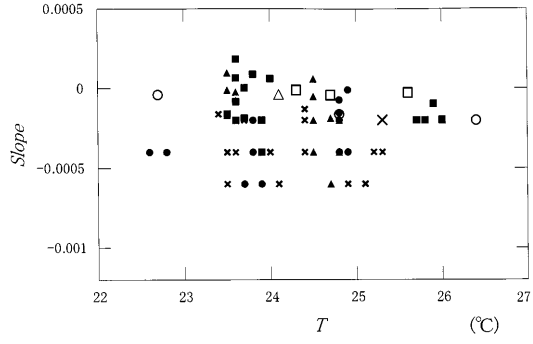

Fig. 6 Slopes of the final equilibrium lines in the rotational relaxations of W29, 0.20 wt%. ○ : "up", 0 G, ×: "down", 0 G, △: "back", 0 G, □: "side", 0 G, ●: "up", 1 G, ×: "down", 1 G, ▲: "back", 1 G, ■: "side", 1 G

"up" and "down" flow directions, this depletion zone of the colloidal particles by sedimentation does not extend to the central area of the cell within 4.5 s in the observation position. This depletion will not occur for the "back" flow direction. The reason for the negative values of the slopes for these three directions is ascribed to the fact that the tail of the rotational relaxation still lasts in the range $t = 4$–4.5 s. On the other hand, the vertical height of the observation cell is so short (5 mm) that depletion does not occur within the observation time.

Since the suspension temperature differs slightly for each experiment, all the data of the slopes observed in this work are compiled in Fig. 6 as a function of suspension temperature. Clearly, experimental errors in the slopes at 1 G were large. The main cause is the significant effect of flow direction in the observation cells as described earlier. We should further note that the convection of the suspension at 1 G is one of the important causes for the large experimental error. Changes in the transmitted-light intensity by the movement of very small impurities such as dust and bubbles, which cannot be seen with the naked eye, are highly plausible in gravity.

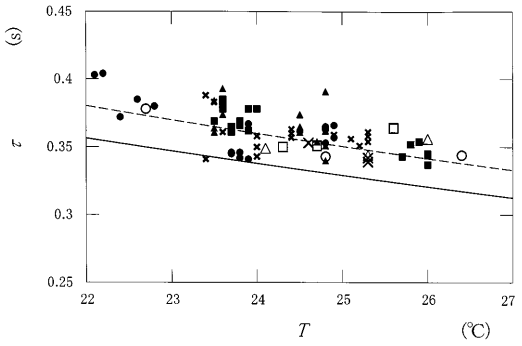

Fig. 7 Rotational relaxation time (τ) of W29, 0.20 wt%.○: "up", 0 *G*, ×: "down", 0 *G*, △: "back", 0 *G*, □: "side", 0 *G*, ●: "up", 1 *G*, ×: "down", 1 *G*, ▲: "back", 1 *G*, ■: "side", 1 *G*. *Solid curve*: calculated from Perrin's equation (D_l = 0 nm), *broken curve*: calculated (D_l = 21 nm)

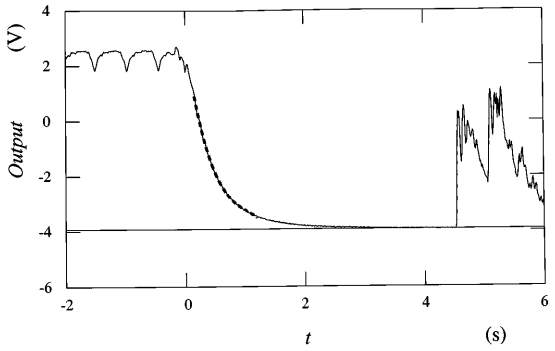

Fig. 8 Rotational relaxation curve of W29 particles at 22.7 °C. At 0 *G*, 0.20 wt%, "up". *Straight line*: linear fitting, *broken curve*: exponential fitting

The relaxation times observed in gravity are shown in Fig. 7. All the solid symbols show the τ values observed at 1 *G*. A decreasing tendency of τ was observed as the suspension temperature increased. Clearly, the observed τ values at 1 *G* scattered rather significantly, which is also explained by the movement of the very small impurities as already described. It should be noted further that the τ values at 1 *G* were about 6% larger than that evaluated theoretically using Eqs. (2)–(6). This difference demonstrates the importance of the electrical double layers formed around the colloidal particles. The broken curve shows the τ values when D_l was taken to be 21 nm. Conductivity measurements of the colloidal suspension gave 36.7 μS/cm (23.3 °C) at ϕ = 0.20 wt%, which corresponds to 2.5×10^4 mol/l KCl and a D_l value of 27 nm. Thus, agreement between the observed and calculated values of D_l at 1 *G* is satisfactory.

Microgravity experiments

Typical transmitted-light intensities observed in microgravity for the "up" flow direction are shown in Fig. 8. t = 0 is the time when the *G* sensor of the free-fall facility detects that $G < 0.1$, and at this point the suspension circulation is stopped. The straight and broken lines are linear and exponential fits, respectively. The strange signal recorded after t = 4.5 s is caused by about 10 *G* application when the capsule is stopped.

The limiting slopes and τ values are obtained from a series of experiments in microgravity. Figure 6 shows the limiting slopes at 0 *G* for "up" (open circles), "down" (large cross), "back" (open triangles) and "side" (open squares), respectively. As described previously, the τ values at 1 *G* were greatly scattered, whereas those at 0 *G* were close to zero irrespective of the flow directions. In microgravity it is clear that no sedimentation of colloidal particles and also no convection of the suspension occur.

The τ values obtained at 0 *G* are compared with those obtained at 1 *G* in Fig.7. Clearly, the τ values in microgravity were not scattered so much compared with those in the normal gravity, and there was no difference between the τ values observed at 0 and 1 *G*. Again, the observed τ values were larger than the theoretical ones due to the significant contribution of the electrical double layers as described earlier. The experimental errors in τ at 0 *G* were smaller than those at 1 *G*. The τ values at 0 *G* were quite insensitive to the flow directions. For more reliable values of τ were observed in microgravity, which again supports the fact that the lack of sedimentation of the colloidal particles, no convection of the suspension and no movement of the impurities raise the reliability of the experimental data significantly.

Acknowledgements Gifu Prefecture and the Space Forum project of the National Space Development Agency of Japan (NASDA) are highly appreciated for their financial support. The authors thank the Micro-Gravity Laboratory of Japan (MGLAB) Co., Toki, Gifu, for the technical support of the free-fall experiments.

References

1. Microgravity Polymers (1986) NASA Conference Publication C-2392, Cleveland, Ohio, June 1985
2. Schiffman RA (ed) (1988) Experimental methods for microgravity materials science research, vol 2, 2nd International Symposium. TMS CD-ROM Library, TMS
3. Schiffman RA (ed) (1992) Experimental methods for microgravity materials science research, vols 4–8, 4–8th International Symposia. TMS CD-ROM Library, TMS
4. Vanderhoff JW, El-Aasser MS, Micale FJ, et al. (1986) PMSE Proc Am

Chem Soc Div Polym Mater Sci Eng 54:584
5. Briskman V, Kostarev K, Leontyev V, Levkovich M, Mashinsky A, Nechitailo G (1997) In: Proceeding of the 48th International Astronaut Congress, Turin, Italy. International Astronaut Federation, pp 1–11
6. Zhu J, Li M, Rogers R, Meyer W, Ottewill RH, STS-73 space shuttle crew, Russel WB, Chaikin PM (1997) Nature 387:883
7. Okubo T, Tsuchida A, Okuda T, Fujitsuna K, Ishikawa M, Morita T, Tada T (1998) Colloids Surf (in press)
8. Okubo T, Tsuchida A, Kobayashi K, Kuno A, Morita T, Fujishima M, Kohno Y (1999) Colloid Polym Sci
9. Cohn EJ, Edsall JT (1943) Proteins, amino acids and peptides. Reinhold, New York
10. Weber G (1953) Adv Protein Chem 8:416
11. Jerrard HG (1959) Chem Rev 59:345
12. Frey M, Wahl P, Benoit H (1964) J Chim Phys 61:1005
13. Wierenga AM, Philipse AP, Reitsma EM (1997) Langmuir 13:6947
14. Okubo T (1987) J Am Chem Soc 109:1913
15. Russel WB, Saville DA, Schowalter (1989) Colloidal dispersions. Cambridge University Press, Cambridge
16. Furusawa K, Hachisu S (1966) J Chem Soc Jpn 87:118
17. Furusawa K, Hachisu S (1963) Sci Light 12:1
18. Furusawa K, Hachisu S (1963) Sci Light 12:15
19. Zocher VH, Jacobson K (1929) Kolloid chem Beih 28:168
20. Perrin F (1934) J Phys Radium 5:497
21. Suda H, Imai N (1985) J Colloid Interface Sci 104:204
22. Hachisu S, Kobayashi Y, Kose A (1973) J Colloid Interface Sci 42:342
23. Pieranski P (1983) Contemp Phys 24:25
24. Okubo T (1988) Acc Chem Res 21:281
25. Okubo T (1993) Prog Polym Sci 18:481